Three Examples of Metamorphic Differentiation

Raymond C. Fletcher

Department of Geological Sciences

University of Colorado at Boulder

Boulder, CO 80309-0399

Table of contents

Previous Section Home Next Section

Fletcher, R.C. 2000. Three Examples of Metamorphic Differentiation. In: Stress, Strain and Structure, A volume in honour of W D Means. Eds: M.W. Jessell and J.L.Urai. Volume 2, Journal of the Virtual Explorer.
ISSN 1441-8126 (Print). ISSN 1441-8134 (CD-ROM).
ISSN 1441-8126 (On-line at www.virtualexplorer.com.au/VEjournal/Volume2).

Abstract

Metamorphic differentiation or segregation of dissolved and reprecipitated minerals in the filling of a boudin gap, in the growth of new grains in a pressure shadow around a cylindrical inclusion, and in limb-to-hinge differentiation in folding may all be expressed in similar terms. A ratio of a rate of deformation arising from dissolution, transport, and precipitation to that due to viscous creep is expressible as the product of two dimensionless quantities. One, the *Bayly Number*, ***B***, incorporates the viscosity, quantities describing the kinetics of dissolution and precipitation and diffusional transport, and a characteristic length scale. Large ***B*** implies significant differentiation during some phase of the structural evolution. A second quantity incorporates dimensions of the current structure, and may change markedly with its evolution.

Previous Section Home Next Section

Introduction

The central theme in Win Mean's research is how fabric in deformed rocks arises and evolves as the rock deforms and recrystallizes. I define *fabric* as a set of attributes of a volume of rock that are statistical in nature. Fabric is abstracted from a more complete description of a rock in a way that discards all information on the spatial relation of its elements, such as grains. Examples are distributions in grain size, shape, or lattice orientation for individual minerals. I define the *structure* as a description in which the spatial information is retained, but limited to elements over a moderate range in scale. A description of a fold structure consists of the configuration of a set of layers. The configuration of grains in each layer is not included, but the distribution of fabric elements in the layer might. The structure of a polycrystalline rock, at the grain scale, involves not only the configuration of the grain boundaries, but also the lattice orientation and composition of each grain, and might include internal grain structures such as kink bands.

One of Win's major insights was that to understand fabric and its evolution, when the elements are grains, structure at the grain scale and the grain-scale processes must both be examined. That is, one cannot understand the processes responsible for the evolution of fabric without appeal to the information contained in the underlying structure. This may now seem obvious. However, much work in structural petrology (e.g., Sander, 1970) has been focussed on the more abstract description based on fabric alone. Vague notions of little practical utility were introduced, one being *componental movements*. I *imagine* that Win, reading about componental movements, decided to go about seeing what, in fact, the detailed motions in a deforming and recrystallizing polycrystalline rock actually were. A second major insight was that to discover what motions *do* take place in a deforming and recrystallizing rock, of all possible, it is necessary to directly observe them. Papers that deal with Win's innovative work based on these two insights include Means (1977, 1980, 1989, 1994), and Means et al. (1984).

To make sense of such observations requires an understanding of kinematics, and Win has made numerous contributions to the structural geology literature in this area (Means, 1976,1990, 1993, 1994; Cobbold et al., 1984). To understand the causative elements that determine the motions, it is necessary to bring in concepts such as stress and constitutive behavior (Means, 1976, 1990).

Much structural geology follows, to a large degree, an approach advocated by Bruno Sander, the Austrian geologist. He commented (Sander, 1970, p. 12): "A clear separation between geometrical and dynamic considerations was maintained by Becker, the American geologist, at a very early date, and he referred to the English physicist Thomson (Lord Kelvin), who says very clearly:

> 'We can see, therefore, that there are many attributes of movement, displacement, and deformation which can be considered independently of force, mass, chemical composition, elasticity, heat, magnetism and electricity; and it is of greatest use to science for such properties to be considered as a first step.' "

I do not know the context of Lord Kelvin's remark. Though much may be learned by observation of natural and experimental examples and from detailed consideration of kinematics, either through experimental observation or interpretation, the *processes* of rock deformation must finally be studied by means of models incorporating mechanics. This necessitates going beyond Lord Kelvin's "first step," and the use of physical and chemical

principles and constitutive postulates not derivable from observation of structure or even of the detailed motions within rocks or analog materials.

Metamorphic differentiation is one example of a process that cannot be adequately addressed purely on the basis of kinematics. Deformation could take place without differentiation, or with variable amounts of it, as seen in natural and experimentally produced examples. The amount of differentiation depends on the value of a physical parameter controlling the rate of deformation, namely, the viscosity, several that control dissolution, transport, and precipitation, and an absolute length scale (see also Bayly, 1996).

In this paper, I present models for three examples in which "pressure-solution" at the macroscopic scale of interest results in "metamorphic differentiation," the separation of one or more minerals from some region in a rock and their segregation in another.

The examples are: (i) the filling of a gap between boudins; (ii) the development of pressure shadows around a stiff inclusion; and (iii) the transfer of a soluble mineral from the limbs of a multilayer fold or crenulation to the hinges. The last is the example to which "metamorphic differentiation" is most generally applied. However, the behavior in all three examples is expressed by results that are similar in form, varying only with the geometry of the structure and the conditions of loading. In each case, dissolution, diffusive transport, and precipitation of a soluble mineral modify the deformation that goes on anyway. The degree to which "differentiation" modifies the deformation may be quantified by the ratio between a rate of deformation ascribable to it and the rate of deformation due to creeping flow. In these examples, and perhaps generally, this ratio is a product of two dimensionless numbers. One contains the physical quantities governing dissolution and precipitation, diffusion, and rock creep; the other is made up of geometric quantities and may change markedly during structural evolution.

For simplicity, the mechanical elements are treated as Newtonian viscous fluids. Dissolution, diffusion, and precipitation take place along discrete interfaces. Hence, the postulate is made that these depend upon an interfacial chemical potential of the solid components, the variation in the equilibrating value of which (Gibbs, 1906; Kamb, 1961) is dominated by a term proportional to the normal stress acting across the interface. This postulate is seemingly in contrast to the use of a continuum formulation by Fletcher (1982), but the latter formulation implicitly follows from a micromechanical model in which the former postulate is applied. The postulate used here may differ in a more fundamental way from continuum approaches of other sorts (e.g., Bayly, 1992, and this volume), although this point is not established at present.

I give results obtained from the mechanical analysis of simple models, but do not provide the details of the analysis, partly to avoid greatly lengthening the paper. As Win has noted (Means, 1990, p. 953; 1994, p. 445), students of structural geology generally do not acquire the background in mechanics required to formulate and analyze such models. Perhaps the results obtained and their potential application to interpretation of natural examples will inspire students (Means, 1991) to study this material. The methods should work well to gain insight into the behavior of natural or analog polycrystalline materials.

Previous Section Home Next Section

Filling of a Bouding Gap

De Paor et al. (1991) described boudinage of dolomite beds in limestone. Several stages in boudin separation are shown in Figure 1. When the boudin gap, Δ, is small, relative to layer thickness, H, the gap is entirely filled by dissolved and reprecipitated calcite from the surrounding limestone. At larger Δ, the weaker limestone begins to flow into the gap and the calcite fill is also deformed. At large Δ, infill is chiefly by flow, and the earlier precipitated calcite is drawn out into a thin sheet within the gap. The sheet thickness increases close to the boudin faces.

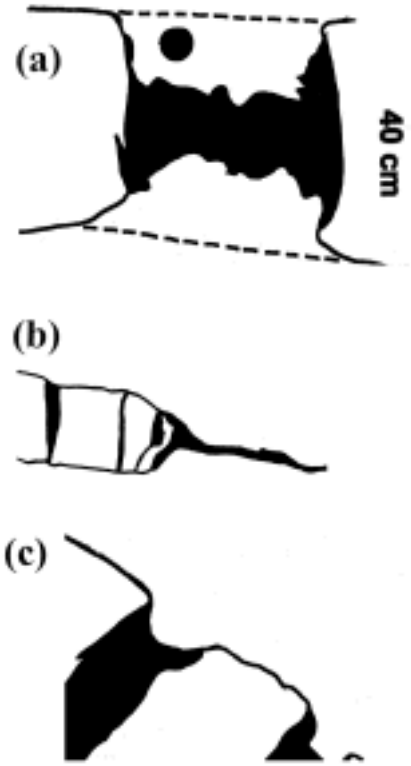

Figure 1. Precipitated calcite (black) in gaps between dolomite boudins in the Rheems Quarry, Rheems, Pennsylvania, from photographs in De Paor and others (1991). The filled black circle in (a) is a lens cap. Filling of the gap wholly by precipitated calcite occurs in the thin cracks in (b). The beginning of partial filling by flow is shown in (c). Filling chiefly by flow is shown in (a). If, in (a), the area of calcite fill is put into a rectangle with length 40 cm and width δ, δ = 12 cm, or about one-third of the total boudin gap. The stretched, initially precipitated calcite fill in (b) indicates large boudin separation.

Thus, two mechanisms contribute to filling the boudin gap. The rate of one is controlled by the rates of dissolution, diffusive transport, and re-precipitation, the other by the rheological behavior of the limestone and the geometry of the boudin gap. The observations indicate that the first mechanism is dominant when $\Delta/H << 1$. At some critical value, Δ^*/H, the two mechanisms contribute equally, and for higher values, the flow of softer rock into the gap dominates, although precipitation against the faces of the boudin may continue to result in the growth of pressure shadows. In examples like those shown in Figure 1, the area of reprecipitated calcite may be cast into the form of a boudin fill of uniform width Δ' and height, H. Then, Δ' is an upper bound on Δ^*, the gap width at which both mechanisms contribute equally. From the examples in Figure 1, Δ' may be estimated to lie between 3 cm and 12 cm. The smaller values are from measurements of gaps the further opening of which has been arrested; H is about 40 cm.

I derive quantitative models for each gap-filling mechanism. Their simultaneous operation is accounted for by the condition that the operative stress is the same. The bulk rate of extension for the mechanism involving dissolution, transport, and precipitation is

$$[D_{xx}]_{ps} = \Omega[2/(W + H)](\sigma_{xx} - \sigma_{zz})V_0 \qquad (1a)$$

where

$$\Omega = [(6MV_0/WH)K]/[(6MV_0/WH) + K] \quad (1b)$$

The diffusive transport coefficient (Robin, 1979) is

$$M \approx (D\xi)(c_0/RT) \quad (1c)$$

where D is the diffusivity in bulk fluid, ξ is the effective thickness of the diffusion path, c_0 is the mean concentration of the dissolved component, R is the gas constant, T is the absolute temperature, and V_0 is the specific volume of the solid phase. W is the length of the boudin, and W/H ≈ 3 – 4. The mechanism is approximated as dissolution along the layer surfaces of the boudin, and diffusive transport along them and a crack between the boudin faces. Diffusion is driven by the gradient in chemical potential of $CaCO_3$ along this path, μ. Dissolution and precipitation are governed by a linear kinetics law of the form

$$d\Delta/dt = 2K(\mu - \mu_{eq}) \quad (2)$$

written here for precipitation onto the *two* surfaces of a single crack in the boudin gap, where μ_{eq} is the equilibrating potential, the variation of which is dominated by the variation in normal stress (Kamb, 1961).

The parameter in (1b) has limiting values, corresponding to diffusion rate-controlling, $K >> 6MV_0/WH$, or kinetics rate-controlling, $6MV_0/WH >> K$. As the absolute scale is reduced, a limit in which kinetics is rate-controlling is always reached, though this will probably not correspond to the natural example. At a large enough scale, diffusion is rate-controlling.

The model for flow into the boudin gap is that for the flow of a viscous fluid between two separating rigid plates (Jaeger, 1962). This approximation is good only if the width of the gap is much less than the layer thickness, or $\Delta/H << 1$. It ignores the external flow that supplies the flux of material into the gap. For this mechanism

$$[D_{xx}]_f \approx (1/4\eta)(\sigma_{xx} - \sigma_{zz})[2\Delta^3/H^2W)] \quad (3)$$

Equality of the two rates of extension at the same stress difference establishes an estimate of Δ^*. The ratio of rates of extension for the two mechanisms is

$$[D_{xx}]_{ps}/[D_{xx}]_f = [4\eta\Omega V_0/(W + H)](H^2W/\Delta^3) = \boldsymbol{B}(H^2W/\Delta^3) \quad (4)$$

The ratio is the product of two dimensionless numbers, ***B***, and a combination of structure dimensions that decreases markedly with boudin separation. Setting the ratio equal to unity

$$\Delta^* = \{\boldsymbol{B}(H^2W)\}^{1/3} \quad (5)$$

Diffusion is rate controlling here, so that

$$\Delta^* = \{24\eta MV_0^2[H/(W + H)]\}^{1/3} \quad (6)$$

Δ^* does not depend on the absolute length scale. That means that Δ^*/H decreases with absolute length scale.

I informally call ***B*** the *Bayly Number*, in acknowledgement of Brian Bayly's extensive contributions (e.g., Bayly, 1988, 1992,1996) to the investigation of the relative roles of diffusive transport and deformation in rock deformation. If ***B*** is small, little differentiation or segregation occurs. From (5), if ***B*** = 1, the transition gap width is of the order of the boudin thickness. However, the approximate models used would break down before such a gap is reached.

Among the parameters controlling the rates of the two mechanisms, the viscosity, η, and the effective diffusion path thickness, ξ, are probably the least well constrained. Using estimates for the parameters, excluding η and ξ, of $D \approx 10^{-5}$ cm^2/s, $c_0 = 3 \times 10^{-5}$ gm/cm^3, $V_0 = 0.368$ cm^3/gm = 36.8 cm^3/mole, $R = 8.3 \times 10^7$ erg deg^{-1} mol^{-1}, T = 400K, and W/H = 3, I have evaluated Δ^* for likely ranges in η and ξ. The result (Figure 2) accommodates not unreasonable values of these for the estimate $\Delta' \approx \Delta^*$.

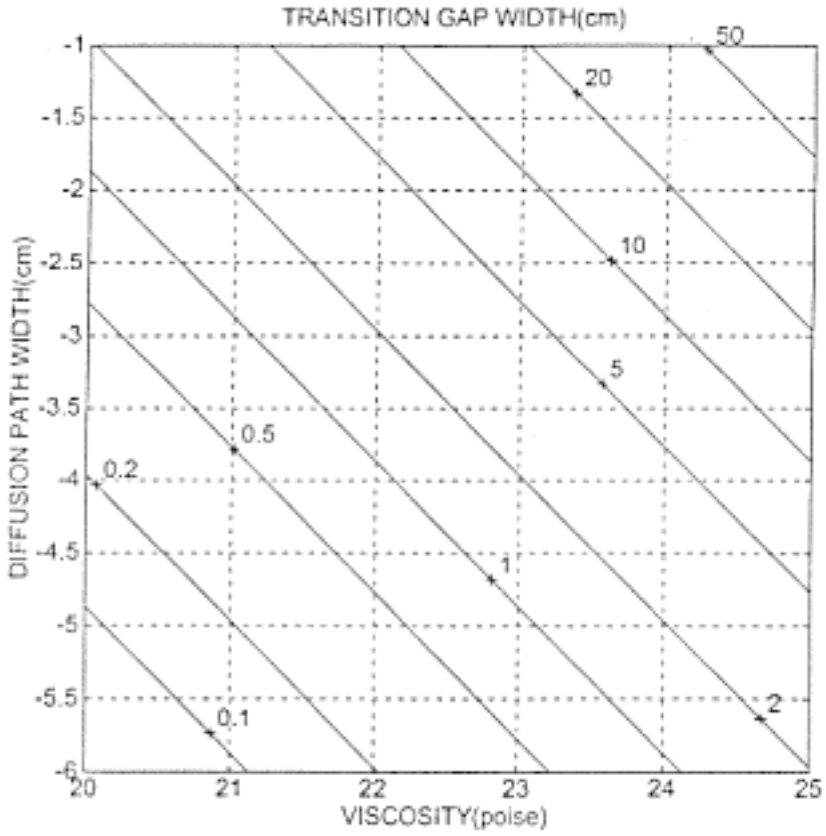

Figure 2. Estimates of transition boudin gap width Δ^* as a function of choices of viscosity, η(poise), and effective diffusion path width, ξ (cm). See text for further discussion.

Using these quantities, $6(D\xi)(c_0/RT)V_0/WH \approx 1.25 \times 10^{-21}\ \xi$ s/cm,

with ξ expressed in centimeters. The kinetic parameter for calcite at 100° C is the much larger quantity $K = 10^{-16}$ s/cm. Hence, diffusion is rate-controlling.

From the computation, the required width of the diffusion pathway, ξ, is rather large for a plausible viscosity. For example, for $\eta = 10^{21}$ Pa-s (10^{22} poise), $\xi = 10^{-3}$ cm for $\Delta^* = 3$ cm. In computing the rate of dissipation in the system due to inflow of soft limestone, the dissipation associated with the flow towards the boudin gap is ignored. If this were included and were quantitatively important, contrary to our postulate, the estimates would be more in line with expectations.

The corresponding estimate of the Bayly Number is $\boldsymbol{B} = 1.15 \times 10^{-22}\, \xi(\text{cm})\eta(\text{Pa–s})$. For $\xi = 10^{-3}$ cm and $\eta = 10^{21}$ Pa-s, this takes the small value $\boldsymbol{B} \approx 10^{-4}$. Hence, even small values of $\boldsymbol{B}$ may be associated with significant segregation. This is because of the large value of the geometric factor, H^2W/Δ^3, which goes to infinity as Δ approaches zero. At $\Delta = 3$ cm, $H^2W/\Delta^3 = 6 \times 10^3$ for the present example.

The model may be used to estimate the variation in stress with gap width needed to open the boudin gap at a specified rate of deformation, or the proportion to which either mechanism contributes to the rate of opening as a function of gap width.

Previous Section Home Next Section

The Growth Of A Mineral Segregation In A Pressure Shadow About A Circular Cylindrical Inclusion In A Newtonian Viscous Fluid

The development of "pressure shadows" about a stiff inclusion is an example of differentiation closely related to the previous. I again assume, in the absence of information to the contrary, that the material forming the pressure shadows bounded by portions of the inclusion surface comes from dissolution over the remaining portions. The case in which dissolution occurs within the host material leads to several interesting problems, discussed in this volume by Brian Bayly (see also Finley, 1996).

Though it would be preferable, for application to natural rocks, if the inclusion were spherical or ellipsoidal in shape, I give here an approximate solution for the simpler problem of an inclusion of cylindrical form with circular cross-section. The flow is plane, with the axis of the inclusion normal to the plane of flow. I expect that consideration of a cylinder, rather than a sphere, would provide insight into the natural phenomenon. This supposition is similar to that taken in the modeling of polycrystalline rock by an analog material consisting of a thin sheet of crystals about one grain thick (Means, 1977, 1980, 1989).

Let the far-field deformation be pure shear in plane flow at rate D_{xx}^{0},

where

$$D_{xx}^{0} = (1/4\eta)(\sigma_{xx}^{0} - \sigma_{zz}^{0}) \qquad (7)$$

Let the inclusion have a viscosity η^*. The x-axis is in the direction of extension, so $D_{xx}^{0} > 0$.

A distribution of dissolution of the host over a portion of the interface and precipitation over the other portion may be written in a way that is formally equivalent to a homogeneous deformation of the inclusion (see also Bayly, this volume). Let D_{xx}^{T*} and D_{zz}^{T*} be the components of a rate of stress-free transformation of the inclusion that is not associated with its viscous deformation. Here, I take the rate of dilation to be zero, to correspond to a net rate of dissolution equal to that of precipitation. The associated radial velocity at the surface of the inclusion is

$$v_r^{T*} = \tfrac{1}{2}(D_{xx}^{T*} - D_{zz}^{T*})a\cos(2\theta) \qquad (8)$$

where a is the radius of the inclusion. A tangential component

$$v_\theta^{T*} = -\tfrac{1}{2}(D_{xx}^{T*} - D_{zz}^{T*})a\sin(2\theta) \qquad (9)$$

has no equivalence in the actual process, although it is formally accounted for in the solution. In this respect, the present model is an approximation.

Associating v_r^{T*} with diffusional transport along the interface, we have

$$v_r^{T*} = -(\partial J_s/\partial s)V_0 = MV_{0\partial}{}^{2}\mu/\partial s^2 \qquad (10a)$$

Separately, associating v_r^{T*} with dissolution and precipitation along the interface

$$v_r^{T*} = K(\mu + \sigma_{rr}*V_0) \quad (10b)$$

The formulation used in the previous example is repeated here, with J_s the interfacial flux, μ the chemical potential of the pressure shadow component in the fluid film, and σ_{rr}* the radial, or normal, component of stress at the circular interface. The arclength is $s = a\theta$, where θ is the angle of the radius vector measured counterclockwise from the positive x-axis. Further,

$$\sigma_{rr}* = \tfrac{1}{2}(\sigma_{xx}* + \sigma_{zz}*) + \tfrac{1}{2}(\sigma_{xx}* - \sigma_{zz}*)\cos 2\theta \quad (11)$$

where σ_{xx}* and σ_{zz}* are the non-zero components of the uniform stress in the inclusion referred to the Cartesian axes.

The relations between the stresses in the inclusion, which are homogenous, those of the far field, and the rate of deformation corresponding to the stress-free transformation have been obtained by an analysis too lengthy for inclusion here. They were derived from a more general solution for an elliptical cylindrical cavity in an orthotropic anisotropic elastic solid (Lekhnitskii, 1963) and the method used in the analysis of an ellipsoidal inclusion in an otherwise uniformly stressed elastic solid (Eshelby, 1957). I found

$$\begin{aligned} &\sigma_{xx}* + \sigma_{zz}* = \sigma_{xx}^0 + \sigma_{zz}^0 \\ &\sigma_{xx}* - \sigma_{zz}* = [2/(1 + \eta/\eta*)](\sigma_{xx}^0 - \sigma_{zz}^0) - [2\eta/(1 + \eta/\eta*)](D_{xx}^{T*} - D_{zz}^{T*}) \end{aligned} \quad (12)$$

Choice of the form

$$\mu = \alpha + \beta\cos 2\theta \quad (13)$$

and its substitution into the equations (10) together with (11) and (12) yield expressions for the desired quantities. In particular

$$D_{xx}^{T*} - D_{zz}^{T*} = [2\,\boldsymbol{B'}/(1 + \boldsymbol{B'})](D_{xx}^0 - D_{zz}^0) \quad (14a)$$

where

$$\boldsymbol{B'} = [2\eta/(1 + \eta/\eta*)](V_0/a)\Omega' \quad (14b)$$

and

$$\Omega' = K(4MV_0/a^2)/(K + 4MV_0/a^2) \quad (14c)$$

A comparison of $\boldsymbol{B'}$ and Ω' with $\boldsymbol{B}$ and Ω of the boudin gap model will show why I have made the present identifications.

Here, the ratio of rates of deformation is between that associated with the pressure shadow and the far field rate. If $\boldsymbol{B'} = 0$, of course, no pressure solution occurs, and a pressure shadow does not form. If $\boldsymbol{B'} = 1$, the equivalent rate of deformation from formation of the pressure shadow is just equal to the far-field value. In essence, interfacial dissolution, transport and precipitation have served to remove the effect of the rigid inclusion from the *local* field of deformation. However, if the inclusion is not rigid, or nearly so, the strain computed from the pressure shadow exceeds the far field value. For $\boldsymbol{B'} > 1$, this is always true. The maximum

rate of deformation associated with the growth of a pressure shadow, when $\boldsymbol{B'} \rightarrow \infty$, is twice the far- field value. The inclusion now looks like a cavity filled with an inviscid fluid at a pressure equal to the negative of the far-field mean stress. The stress difference in the inclusion is

$$\sigma_{xx}^* - \sigma_{zz}^* = [2/(1 + \eta/\eta^*)][1/(1 + \boldsymbol{B'})](\sigma_{xx}^0 - \sigma_{zz}^0) \qquad (15)$$

This becomes reduced as $\boldsymbol{B'}$ increases, the limiting value being zero. These results suggest that the use of pressure shadows to estimate strain, and perhaps "strain history," need to be carefully examined.

I speculate that if pressure solution acts to produce a pressure shadow about an inclusion that is much larger than the host grains, operating at the grain scale, it would lead to a very substantial rate of deformation within the host. The same argument would apply to the filling of a boudin gap, where, moreover, the disparity between the scale of the boudin and that of the grains is very much greater. One might then wonder how the "driving force" in terms of a variation in normal stress large enough to drive pressure solution at the much larger scale would come about. The known result for the boudin, that the gap being filled is a crack, suggests that pressure shadows around stiff inclusions may also be bound by an interfacial crack on one side. The mechanics of the process would then be somewhat different from that considered here.

Previous Section Home Next Section

Interfacial Dissolution, Diffusion, And Precipitation In A Viscous Multilayer

The term "metamorphic differentiation" is usually restricted to the striking compositional layering that develops under certain circumstances between the hinge and limb regions of small-scale folds in foliated quartz/phyllosilicate rocks (Nicholson, 1966; Gray and Durney, 1979). Durney (1979) presented a model for its development. I re-analyze his model, but only for the early stage of fold development. As in the previous examples, one effect of dissolution, diffusion, and precipitation is to reduce the magnitude of the stress heterogeneity driving it. This leads to a qualitatively different result from the approximation in which this feedback is ignored, as in Durney's treatment. Also, the stress distribution in such a multilayer is substantially different from the homogeneous stress that Durney assumed to estimate the rate of differentiation. The continuous layers of Durney's model simulate the resistance of micas to bending, the likely importance of which was pointed out by Robin (1979).

The analysis follows the approach described in Johnson and Fletcher (1994). The multilayer is composed of layers of equal thickness, H, and viscosity η. The layers are separated by weak interfaces on which the slip rate, $\Delta\{v_s\}$, is set proportional to the resolved shear stress, σ_{ns}, where s and n are local coordinates parallel and normal to the interface. Treating the interfaces as thin layers of thickness δ^* and viscosity η^*,

$$\Delta\{v_s\} = (\delta^*/\eta^*)\sigma_{ns} \qquad (16)$$

The folding is vertically repetitive, with vertical axial planes, and occurs in shortening parallel to the mean orientation of the layers. Each interface is described by the locus, relative to the mean mid-plane of the layer,

$$z = H/2 + \boldsymbol{A}\cos(\lambda x) \qquad (17)$$

where $\lambda = 2\pi/L$, and L is the fold wavelength.

A measure of the rate of differentiation is the rate of growth in the thickness of the "saddle reefs" into which, in the model, the phase transported from the fold limbs precipitates. This is just the difference in normal velocities, $\Delta\{v_n\}$, evaluated at a hinge. The rate of thickening of the layer, excluding the saddle reef, at the hinge is $-D_{xx}H$. The ratio $-\Delta\{v_n\}/D_{xx}H$ is a measure of the relative contributions of differentiation and layer deformation to the bulk rate of elongation along the hinge. From the analysis, I obtain

$$-\Delta\{v_n\}/D_{xx}H \cong \{(4\eta V_0/H)\Omega''/[1 + (4\eta V_0/H)\Omega'']\}[(2 + \theta^*/2)/(k^2/3 + \theta^*)](\lambda\boldsymbol{A})^2\cos(2\lambda x) \qquad (18a)$$

where

$$\Omega'' = K(MV_0/\lambda^2)/[K + (MV_0/\lambda^2)] \qquad (18b)$$

$k = 2\pi H/L$ is a dimensionless wavenumber, and $\theta^* = (\eta^*/\eta)(H/\delta^*)$. Comparison with the result for the pressure shadow suggests the identification of the Bayly Number with the

quantity

$$\boldsymbol{B''} = (4\eta V_0/H)\Omega'' \tag{19}$$

The expression (18a) thus also contains the factor [$\boldsymbol{B''}/(1 + \boldsymbol{B''})$] times another dimensionless quantity containing θ^* and k, times the square of the maximum limb dip (in radians). As in the model for grain growth in a pressure shadow, the factor in $\boldsymbol{B''}$ embodies the principle of "saturation," with reduction in the driving term as $\boldsymbol{B''}$ increases. Thus, this factor varies between zero and unity as $\boldsymbol{B''}$ ranges from zero to infinity.

Since differentiation only enters to second-order in the limb dip, $\lambda\boldsymbol{A}$, it cannot enter into the wavelength-selection process. The rate of amplification is

$$d\boldsymbol{A}/dt \cong -D_{xx}\boldsymbol{A} - 2D_{xx}\boldsymbol{A}/(k^2/6 + \theta^*) \tag{20}$$

In (20) and (18a), the exact result has been reduced to leading terms in k for $k << 1$, appropriate for large wavelength to layer thickness ratio, $L/H >> 1$. The approximations hold to terms $\sim (\lambda\boldsymbol{A})^2$, or up to limb-dips $\approx 10^o - 20^o$, above which both rates increase more slowly with limb-dip.

Using (18a) and (20), I have determined the thickness of "saddle reefs", or the amount of differentiation, as a function of limb dip. Consider the limiting case $\theta^* = 0$, in which layer interfaces are frictionless. Let $\tau = t/t^*$ be a dimensionless time, with $t^* = 1/[(12/k^2)|D_{xx}|]$. In the approximation that the basic-state shortening need not be accounted for, appropriate if fold amplification is rapid, or $t^* << 1/|D_{xx}|$, (20) yields

$$\lambda\boldsymbol{A}(\tau) = \lambda\boldsymbol{A}(0)e^{\tau} \tag{21}$$

where $\boldsymbol{A}(0)$ is the initial amplitude. If $n(\tau)$ is the thickness of the saddle reef at the hinge, from (18a), (19), and (21)

$$d[n(\tau)/H]/d\tau = t^*[\Delta\{v_n\}_{x=0}]/H = (\tfrac{1}{2})[\boldsymbol{B''}/(1 + \boldsymbol{B''})](\lambda\boldsymbol{A})^2 \tag{22}$$

Integrating (22)

$$n(\tau)/H = (\tfrac{1}{4})[\boldsymbol{B''}/(1 + \boldsymbol{B''})](\lambda\boldsymbol{A})^2 \tag{23}$$

The thickness of the saddle reefs, or the amount of differentiation, is a function only of the Bayly Number and the limb dip. Consequently, $\boldsymbol{B''}$ can be estimated from field observations of n/H versus limb dip. The function (23) is plotted in Figure 3 for dips up to 45° , probably beyond where it gives a good approximation, for small ($\boldsymbol{B''} = 0.1$), intermediate ($\boldsymbol{B''} = 1$), and infinite values of $\boldsymbol{B''}$. The limb dip at which the approximation breaks down is that dip at which the folds no longer appear sinusoidal.

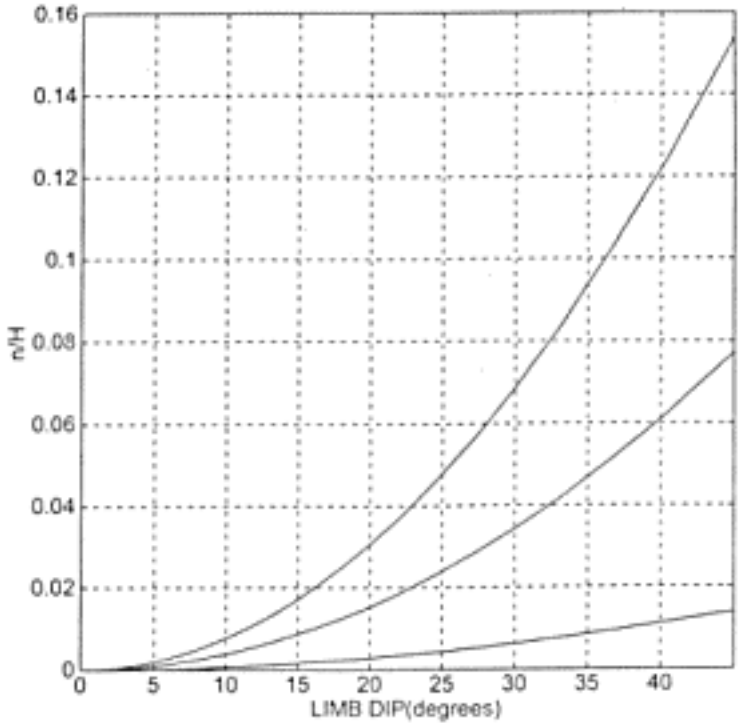

Figure 3. Amount of differentiation, as measured by the ratio of the thickness of a saddle reef to the layer thickness, n/H, as a function of limb dip in a symmetric crenulation, for Bayly Numbers B'' = 0.1, 1, and ∞ .

Previous Section Home Next Section

Discussion

In the examples, I focussed on the amount of mineral segregation in a structure, and its dependence upon the controlling physical and chemical parameters – including the geometry of the structure. The models also provide a complete description of the motions, for example, the velocity and strain fields for the material within the boudin gaps and that within the material around the stiff inclusion (see also Kenkmann and Dresen, 1998).

The structures considered are far simpler than that of a three-dimensional polycrystalline rock. They are simplified versions of the natural structures modeled. The physical and chemical behavior is simplified from what might occur in nature. The simplifications allow me to carry out an analysis of the process by elementary means. If warranted, especially to interpret a good set of field data, a refined model might be formulated and treated by a more laborious analytical or numerical approach (for example, see Kenkmann and Dresen, 1998). The structures treated are not as complex and varied as those in Win's experiments with deforming and recrystallizing polycrystals; yet they have a resemblance to them. In this respect, I have approached the next step, to understand the underlying physics and chemistry of processes in a polycrystalline rock and the evolution of its fabric.

Although it is conventional to speak of "pressure shadows" (Etchecopar and Malavielle, 1987), a reviewer has pointed out two problems with this usage. First, what one observes is a mineral segregation; the stress inhomogeneity is no longer present. Second, the magnitude of the stress inhomogeneity operative when the mineral segregation formed is, as the present results show, proportionately reduced the more prominently developed the segregation, for comparable bulk strain. *When there is no segregation, because of sluggishness of transport or kinetics, all other things being equal, the pressure shadow has maximal magnitude.* A third problem, as with the term "pressure-solution," is that the *pressure*, or negative of the mean stress, is not always the stress quantity whose gradient drives the transport. In the present case, that quantity is the local interfacial normal stress.

The same reviewer also pointed out that the present formulation involves the somewhat paradoxical choice of concentrating dissolution, transport, and precipitation at the boundaries of objects – boudins, porphyroblasts, and folded layers – the dimensions of which are several orders of magnitude larger than the grain scale. It would seem more plausible that such processes, because of scale dependence – especially in diffusive transport, would operate much more efficiently at the grain scale, and, thus, that in most cases the transport of material at a much larger scale would be "short-circuited." This idea has also occurred to me and to others. Observations are generally in support of transport at the larger scale, as in the present models. Of course, in the case of boudin separation, there is no alternative. The same issue also enters in "pressure-solution", in which discrete solution seams (or stylolites) dominate over any pervasive grain-scale process. The suggestion is that large, continuous surfaces behave differently from grain interfaces. As the reviewer suggested, this may have substantial importance in treating all types of transport in rock. Clearly, interconnected cracks will dominate in fluid flow if the grain-scale permeability is sufficiently low. In diffusive transport, intergranular surfaces may be substantially tighter than larger surfaces. Equivalent diffusive transport lengths for two surfaces with effective "gaps" of δ_1 and δ_2 will have the ratio

$$L_1/L_2 = [\delta_1/\delta_2]^{½}$$

As with solution seams, it may also be that these larger surfaces are crack-like in their behavior.

Acknowledgements

NSF Grant EAR 95-26983 to L. B. Goodwin and R. C. Fletcher supported this research. Reviews by Ron Vernon and an anonymous reviewer were helpful.

Previous Section Home Next Section

References

Bayly, B., Piezochemistry, Bulletin of the Geological Institutions of the University of Uppsala, 14, 25 – 29, 1988.

Bayly, B., Chemical change in deforming materials, Oxford University Press, 1992.

Bayly, B., Stress and diffusion in a one-component viscous continuum, in Diffusion and Stresses (D.L. Beke and I. A. Szabo, editors), Defect and Diffusion Forum, 129 – 130, 281 – 288, 1996.

Cobbold, P. R., W. D. Means, and M. B. Bayly, Jumps in deformation gradients and particle velocities across propagating coherent boundaries, Tectonophysics, 108, 283 – 298, 1984.

De Paor, D. G., C. Simpson, C. M. Bailey, K. J. W. McCaffrey, E. Beam, R. J. W. Gower, and G. Aziz, The role of solution in the formation of boudinage and transverse veins in carbonate rocks at Rheems, Pennsylvania, Geological Society of America Bulletin, 103, 1552 - 1563, 1991.

Durney, D. W., A theory of mass-transfer-buckling deformation in finite amplitude sinusoidal multilayers, in Mechanisms of Deformation and Fracture, K.E. Easterling (ed.), Pergamon Press, Oxford, U. K., 393 – 405, 1979.

Eshelby, J. D., The determination of the elastic field of an ellipsoidal inclusion and related problems, Proceedings of the Royal Society of London, Series A, 241, 376 – 396, 1957.

Etchecopar, A., and J. Malavielle, Computer models of pressure shadows: a method for strain measurement and shear sense determination, Journal of Structural Geology, 9, 667 – 677, 1987.

Finley, S. G., Diffusion-enhanced deformation of a circular inclusion, in Diffusion and Stresses (D. L. Beke and I. A. Szabo, editors), Defect and Diffusion Forum, 129 – 130, 281 – 288, 1996.

Fletcher, R. C., Coupling of diffusional mass transport and deformation in a tight rock, Tectonophysics, 83, 275 – 291,1982.

Gibbs, J. W., On the equilibrium of heterogeneous substances, in Collected Works of J. Willard Gibbs, Yale University Press, New Haven, Connecticut, 1906.

Gray, D. R., and D. D. Durney, Crenulation cleavage differentiation: implications of solution-deposition processes, J. Structural Geology, 1, 73 – 80, 1979.

Jaeger, J. C., Elasticity, fracture and flow: with engineering and geological applications, Methuen and Company Limited, London, 212 pp., 1962.

Johnson, A. M., and R. C. Fletcher, Folding of a Viscous Layer: Columbia University Press, 1994.

Kamb, W. B., On the thermodynamic theory of nonhydrostatically stressed solids, J. Geophysical Research, 66, 259 – 271, 1961.

Kenkmann, T., and G. Dresen, Stress gradients around porphyroclasts: paleopiezometric

estimates and numerical modelling, Journal of Structural Geology, 1998.

Lekhnitskii, S.G., Elasticity of an Anisotropic Elastic Body, Holden–Day, San Francisco, 404 pp., 1963.

Means, W.D., Stress and strain: basic concepts of continuum mechanics for geologists, Springer Verlag, New York, 339 pp., 1976.

Means, W. D., A deformation experiment in transmitted light, Earth and Planetary Science Letters, 35, 169 – 179, 1977.

Means, W. D., High temperature simple shearing fabrics: a new experimental approach, Journal of Structural Geology, 2, 197 - 202, 1980.

Means, W. D., Synkinematic microscopy of transparent polycrystals, Journal of Structural Geology, 11, 163 – 174, 1989.

Means, W.D., Kinematics, stress, deformation and material behavior, Journal of Structural Geology, 12, 953 – 971, 1990.

Means, W.D., Opinion: a time for teaching teachers, Geology, 19, 1155, 1991.

Means, W.D., Elementary geometry of deformation processes, Journal of Structural Geology, 15, 343 – 349, 1993.

Means, W.D., Rotational quantities in homogeneous flow and the development of small scale structure, Journal of Structural Geology, 16, 437 – 445, 1994.

Means, W.D., and Y. Park, New experimental approach to understanding igneous texture, Geology, 22, 323 – 326, 1994.

Means, W. D., P.F. Williams, and B.E. Hobbs, Incremental deformation and fabric development in a KCl/mica mixture, Journal of Structural Geology, 6, 391 – 398, 1984.

Nicholson, R., Metamorphic differentiation in crenulated schists, Nature, 209, 68 – 69, 1966.

Robin, P.-Y. F., Theory of metamorphic segregation and related processes, Geocim. Et Cosmochim. Acta, 43, 1587 – 1600, 1979.

Sander, B., An introduction to the study of fabrics of geological bodies (English translation), Pergamon Press, Oxford, U. K., 641 pp., 1970.

Previous Section Home Next Section